academicJournals

Vol. 12(7), pp. 77-88, 17 February, 2018
DOI: 10.5897/JMPR2018.6561
Article Number: 4511CAE56237
ISSN 1996-0875

http://www.academicjournals.org/JMPR

Journal of Medicinal Plants Research

Full Length Research Paper

Quantitative proteomic analysis of Isorhamnetin treatment in human liver cancer cells

Runhuan Fei[1] and Haiyan Wei[2*]

[1]Department of Gastroenterology, Southwest Hospital, Third Military Medical University, Gaotanyan Street 29, Shapingba District, Chongqing, People's Republic of China.
[2]School of Health and Biomedical Sciences, RMIT University, Melbourne, Australia.

Received 26 January, 2018; Accepted 23 February, 2018

Isorhamnetin (Iso) exhibits antitumor effects in promyelotic leukemia and lung cancers. However, its effect in liver cancer is not clear. This study explored the effects of Iso in human liver cancer cells and profiled the differential proteins upon Iso treatment, which contributes to a better understanding of its anticancer mechanisms. Stable isotope labeling with amino acids in cell culture-mass spectrometry: ESI-Iontrap (SILAC-MS) was used to study the differentially proteomic profile of Iso-treated HepG2 cells. Iso inhibits HepG2 cell proliferation in a dose-dependent manner. A total of 84 proteins are identified, among which 7 proteins were up-regulated while 77 proteins were down-regulated. Iso inhibits HepG2 cell proliferation by the induction of apoptosis and the inhibition of protein synthesis of human liver cancer cell.

Key words: Isorhamnetin, Stable Isotope Labeling with Amino Acids in Cell Culture (SILAC), differential proteomic profile, HepG2 cells.

INTRODUCTION

Isorhamnetin (Iso) is a flavonol extracted from the herbs: *Ginkgo biloba* Linne and *Persicaria thumbergii* H. Gross (Ma et al., 2007; Lee et al., 2008). Besides its cardiovascular protective effect, Iso has been demonstrated to exhibit remarkable anti-tumor effects in a range of human cancers. For example, Iso was found to have anti-proliferation effects in lung cancer cells *in vitro* and *in vivo*, by down-regulation of oncogenes and up-regulation of apoptotic genes (Manu et al., 2015). A clinical trial examining the roles of diet in preventing colorectal adenoma recurrence found that Iso-rich diet was connected with a reduced risk of advanced adenoma recurrence (Bobe et al., 2008). Another paper reported that supplementing the diet with Iso remarkably decreased colorectal tumorigenesis in the mice (Saud et al., 2013). Iso affected cell proliferation, cell death, and cell cycle of human colon cancer cell: HCT-116 suggesting its possible therapeutic role in human colon cancer (Jaramillo et al., 2010). Furthermore, Iso was shown to present significant anti-tumor effects in gastric cancer, breast cancer and skin cancer (Manu et al., 2015; Li et al., 2015; Hu et al., 2015; Ramachandran et al.,

*Corresponding author. E-mail: lovelouise2002@gmail.com. Tel: +61-3-99257376.

2012; Kim et al., 2011).

Liver cancer is the leading cause of cancer-related death in China and the survival benefit of current therapeutic drugs for liver cancer is unsatisfied. In addition, previous study showed that quercetin can suppress the growth of liver solid tumor in murine model (Yuan et al., 2006). As the metabolite of quercetin which contributes its anti-cancer functions, Iso has been shown to induce apoptosis in human HL-60 cells more effectively than quercetin *in vitro* (Hibasami et al., 2005). *In vivo* study conducted by Lee et al. (2008) revealed that Iso significantly suppressed Lewis lung cancer growth at a dose that is at least one order of magnitude lower than quercetin by i.p. injection (Lee et al., 2008). These results support that the anti-cancer effect of quercetin may in large part be mediated by Iso (Shimoi et al., 2003; Hibasami et al. 2005; Park et al., 2005; Lee et al., 2008). Previous study showed that quercetin can suppress the growth of liver solid tumor in murine model (Yuan et al., 2006). Iso is probably more effective in liver cancer than quercetin itself since it was reported that the metabolite of quercetin which contributed its anti-cancer functions (Manach et al., 1998; Morand et al., 1998). Therefore human hepatoma cell line (HepG2) was chosen to study the anti-tumor effects of Iso. Stable isotope labeling by amino acids in cell culture (SILAC) combined with mass spectrometry (MS) analysis provides a powerful tool to identify and quantify complex protein samples (Zhu et al., 2002; Ong et al., 2002; Ong et al., 2003). Compared with traditional 2-DE technique, it obtains more abundant quantitative information and has been used more extensively than ever (Sun et al., 2008; Pan et al., 2009; Prokhorova et al., 2009). In SILAC experiments, one cell population is grown in the normal medium with normal (light) amino acid while another population in the same medium with isotopic (heavy) amino acid, for example labelling medium. Cell features, such as cell morphology, cell doubling time, and cell differentiation of the two populations are same. Therefore the intensity ratio of the pair of “light” and “heavy” peaks in the peptide mass spectrum could reflect protein quantitative level under different conditions (Ong et al., 2002).

Here we found that Iso is able to inhibit HepG2 cell proliferation in a dose-dependent manner. Then we applied SILAC-ESI Iontrap technique to profile the proteomic picture of HepG2 cells treated with Iso. Totally 84 proteins changed after the treatment with 50 μM Iso for 48 h. Revealing the differential proteins caused by Iso treatment will contribute to a better understanding of its anticancer mechanisms in liver cancer.

MATERIALS AND METHODS

Iso was a gift from Chengdu Di Ao pharmaceutical group. Dimethyl sulfoxide (DMSO), 3-(4,5-dimethyl-2-thiazolyl)-2,5-diphenyl-2H-tetrazolium bromide (MTT) was purchased from Sigma Chemical Corporation. SILAC^{TM} protein identification and quantitation medium kit with $^{13}C_6$-L-Lysine (*Lys), RPMI1640 and fetal bovine serum (FBS) were obtained from Invitrogen Corporation.

Cell culture and labelling

HepG2 was obtained from the American Type Culture Collection (ATCC) and cultured in RPMI1640 with 10% dialyzed FBS, antibiotics and 0.1 mg/ml $^{13}C_6$-L-Lysine, 0.1 mg/ml $^{12}C_6$-L-Arginine (labelling medium) at 37°C under 5% CO_2. The medium was replaced every 2-3 days, and cells were passaged until 80-90% confluency. β-actin protein was used to check the labelling efficiency by ESI-Quad-TOF. Cells were passaged at least 20 generations to obtain 95% labeling efficiency.

MTT assay

HepG2 cells were seeded into a 96-well plate at a density of 1×10^4/well. On the next day, the plate was added with various concentrations of Iso (158, 52.67, 17.56, 5.85, 1.95, 0.65, 0.22μM) and incubated at 37℃ under 5% CO_2 for 48 h. Each concentration repeated 4 times. Then, 10 μL MTT (5 mg/ml) was added. After 2-3 h, the medium was removed and 100 μL DMSO was added to dissolve formazan precipitate for 10 min. The absorbance at 570 nm was measured on a spectra max MS (MDC, Sunnyvale, CA, USA). Cell viability was calculated as a percentage of viable cells in Iso treated group versus untreated control by the following equation. Cell viability = [OD (Iso)-OD (blank)] / [OD (control)-OD (blank)].

Sample preparation and in-gel digestion

The labelled cells were incubated in the labelling medium containing 50 μM Iso, while the control cells were grown in the normal RPMI1640 medium. Iso treated cells and control cells were collected after 48 h, followed by 3 times wash with PBS. Total protein was extracted with RIPA buffer [10 mM Tris-Cl (pH 8.0), 1 mM EDTA, 0.5 mM EGTA, 1% Triton X-100, 0.1% sodium deoxycholate, 0.1% SDS, 140 mM NaCl, protease inhibitor cocktail]. Protein concentration was determined by Pierce BCA Protein Assay Kit (Rockford, IL, USA). Same amount of protein from each sample were mixed, and separated on a 12% SDS-PAGE followed by Coomassie Blue R250 staining. The lanes were excised horizontally into 20-25 sections. The sections were cut into small pieces and subjected to in-gel tryptic digestion with mass spectrometry grade trypsin (Promega, Madison, WI, USA) as described (Patrick et al., 2004).

MS analysis and protein quantification

The incorporation of $^{13}C_6$-L-Lysine into β-actin protein was detected by ESI-Quad-TOF system, including a nano-ultra performance liquid chromatography and a quadrupole time-of-flight tandem mass spectrometer (UPLC-Q-TOF, Waters, USA) coupled with the electrospray ionization (ESI) source. Peptides were re-dissolved in 50% acetonitrile (ACN)/0.1% trifluoroacetic acid (TFA) and analyzed with reverse phase liquid chromatography followed by tandem mass spectrometry (LC-MS/MS). The MS/MS data (pkl files) acquired by ProteinLynx V2.25 software (Waters) was analyzed with Mascot 2.0 program (MatrixScience Ltd., London).

HepG2 cells upon Iso treatment was analyzed by Agilent 1100 HPLC-Chip/MS system. The peptide mixture (7 μL in 0.5% TFA solution) was first concentrated and washed at 4 μL/min in 40 nL enrichment column (Agilent Technologies Chip), with 5% acetonitrile as eluent. The sample was then fractionated on a C18 reverse-

phase capillary column (75 µm × 43 mm in the Agilent Technologies Chip) at a flow rate of 300 nl/min. Solvent A was 0.1% formic acid and solvent B was acetonitrile with 0.1% formic acid. The gradient of the analytical pump started with 5% B, reached 20% B after 2 min and 45% B after 10 min, and 75% B after 2 min. One minute later solvent B was 95% B for 4 min, then it was set back to 5% with a post run time of 5 min at 5% B.

Elution was monitored on the mass spectrometers with a splitting device. Peptides were analyzed using data-dependent acquisition of one MS scan followed by MS/MS scans. An Agilent 6330 Ion Trap LC/MS was used for MS and MSn data acquisition. The ion trap analysis was performed in positive mode. The drying gas flow was 3 L/min of nitrogen. The drying gas temperature was 325ºC. Capillary voltage was set at -2050 V with an endplate offset of -500 V. Skimmer was at 40 V, capillary exit was 95.8 V and trap drive was 88.1 V. Scan mode was std/Enhanced. Scan range was 300-1600 m/z (MS) and 300-1600 m/z (MS/MS).

Ion Charge Control (ICC) parameters were Target of 500,000; maximum accumulation time of 150 m; Averages was 2.

Automatic MS2 conditions were number of precursors: 3; Active exclusion: on, exclude after 2 spectra, release after 1 min; Abs. threshold auto MS2 was 500,000; Rel. threshold auto MS2 was 5%.

Data analysis

Spectrum mill MS proteomics workbench version A.03.03 was used, which is a collection of tools for high throughput processing of MS and MS/MS spectra.

Data was extracted with the following parameters: MH^+ 600-4000 Da, scan time range from 0-300 min, sequence tag length >1, Maximum (Z) is set as 3, and minimum MS S/N is 25. Tick the option: find ^{12}C.

The MS/MS search was governed by the following parameters: batch size: 81, max reported hits: 5, database: ipi.HUMAN.v3.43.fasta, digest: trypsin, maxium missed cleavages: 2, protein PI: from 3 to 10, carbamidomethylation (C) in fixed modifications, minimum scored peak intensity: 50%, instrument: Agilent ESI ion trap, masses are monoisotopic, precursor mass tolerance:±2.5Da and product mass tolerance:±0.6 Da. Maximum ambiguous precursor charge was 3. At the same time, the reversed database scores are determined automatically with Spectrum mill MS proteomics workbench version A.03.03 (Agilent Technologies).

Protein abundance was expressed as a ratio of the peak intensity of the fragment ions from the labeled versus the unlabeled peptides. Ratios were calculated from the average of all quantified peptides for a single protein. We filtered peptides by peptide score >6, %SPI>70%. We defined the cut-off ratio value of 1.8 which is at least 2.5 times the average standard variation of all quantified proteins. In other words, only the quantified proteins, with ratio over 1.8 or below 0.8, were defined as the significantly changed proteins. Subcellular location and functional analysis were performed according to component and process annotation in Gene Ontology (GO, www.geneontology.org).

Validation of some differential protein expression with real-time fluorescence quantitative RT-PCR and Western blotting

Real-time fluorescence quantitative RT-PCR

HepG2 cells were seeded in a 6-well plate (1 x 10^6 cells/well) and cultured for 24 h in RPMI1640 medium supplemented with 10% FBS followed by a further 48 h culture with 50 µM Iso. Total RNA isolated from the control and treated cells using acid guanidinium thiocyanate/phenol/chloroform was amplified by real-time PCR using an i-Cycler System (Bio-Rad, Hercules, CA, USA) with Prime SYBR premix Ex Taq and PrimeScript RT reagent kit (Takara, Otsu, Shiga, Japan). All samples were investigated in triplicate. Primers used were:

H1b: Forward: 5'-AGAGCCCTAAGAAGGCCAAG-3'
Reverse: 5'-CTACTTCTTTTTGGCAGCCG-3'

HSP90: Forward 5'-GAGGGAGTAATGGCAGGACA-3'
Reverse: 5'-TTAGAACCCGATCCAACAGC-3'

RBMX: Forward 5'-TCGCCCTCGTTGCGCAGTAG-3'
Reverse 5'-CGGTGAGTCGGAGGGGTGACAA-3'

Cdk2: Forward 5'- CACCCATGAGGTGACTCGCCG-3'
Reverse 5'-CAGGGCTGCCTTGGCCGAAA-3'

18S rRNA: Forward 5'-TACCTACCTGGTTGATCCTG-3'
Reverse 5'-GGGTTGGTTTTGATCTGATA-3'

Dissociation curves were examined to ensure the absence of primer dimers. Amplified products were resolved by electrophoresis on 2% agarose gels to confirm a single band. The amplification efficiency was generated from standard curves using serial diluted cDNA templates. The cDNAs were quantified by taking 18S rRNA as the internal reference with results expressed as levels relative to controls.

Western blotting analysis

HepG2 cells were seeded in a 6-well plate (1x10^6 cells/well) and cultured for 24 h in RPMI1640 medium supplemented with 10% FBS followed by a further 48 h culture with 50 µM Iso. Total cell protein was extracted with RIPA buffer [10 mM Tris-Cl (pH 8.0), 1 mM EDTA, 0.5 mM EGTA, 1% Triton X-100, 0.1% sodium deoxycholate, 0.1% SDS, 140 mM NaCl, protease inhibitor cocktail]. The extracts (30 µg) were separated by 12% SDS-PAGE, and transferred onto PVDF membranes (Millipore, Bedford, MA, USA). Membranes were incubated with anti-H1b antibody (1:200, Cell Signaling Technology, Beverly, MA, USA) or anti-Cdk2, RBMX antibody (1:500, Abcam, Cambridge, UK), and then with anti-rabbit IgG conjugated with horseradish peroxidase (1:5000, Cell Signaling Technology, Beverly, MA, USA). Immuno-reactive bands were detected by Pierce ECL detection system (Rockford, IL, USA).

RESULTS

$^{13}C_6$-L-Lysine labelled HepG2 cells are identified by detecting labelling efficiency

The labelling efficiency of HepG2 cells was assessed by detecting $^{13}C_6$-L-Lysine in the peptides of the housekeeping protein: β-actin. Two lysine-containing peptide pairs: the light isotope (m/z 590.3096, 3+) and the corresponding heavy one (m/z 592.3268, 3+) as shown in the Figure 1A; the light (m/z 978.4738, 3+) and the heavy (m/z 980.5278, 3+) in the Figure 1B had a mass difference of 2 Da in ESI-Quad-TOF MS. Increased $^{13}C_6$-L-Lysine was paralleled with decreased $^{12}C_6$-L-Lysine level in β-actin protein during cell labelling. HepG2 cells were regarded successfully labelled when the metabolic labelling of $^{13}C_6$-L-Lysine in β-actin protein reached above 95%.

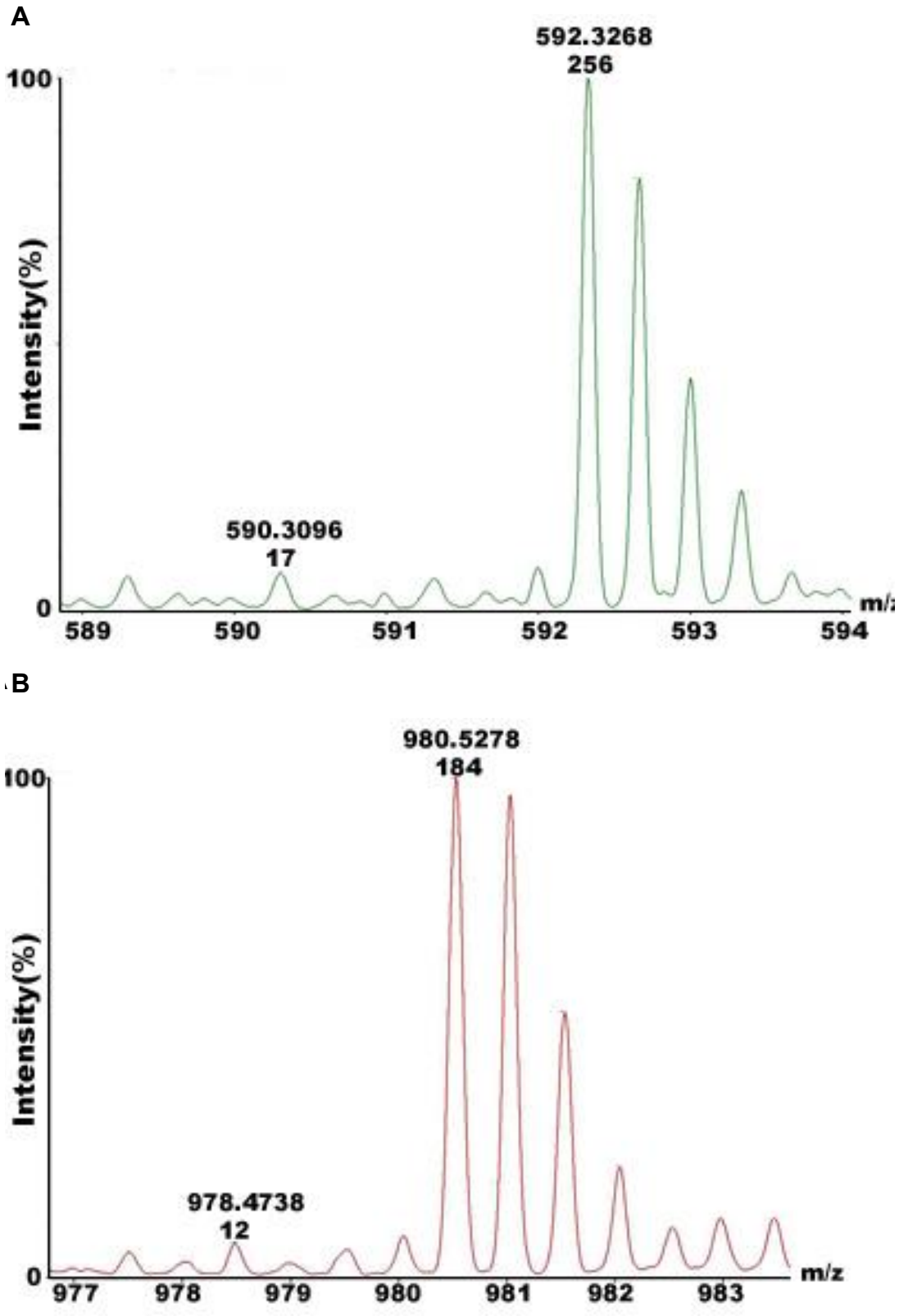

Figure 1. Incorporation of $^{13}C_6$-L-Lysine in β-actin protein of HepG2 cells after about 20 passages. Two lysine-containing peptide pairs: the light isotope (m/z 590.3096, 3+) and the corresponding heavy one (m/z 592.3268, 3+) in A.; the light (m/z 978.4738, 3+) and the heavy (m/z 980.5278, 3+) in B were monitored with the time. HepG2 cells are regarded successfully labelled when heavy/light peak ratio reached above 95%.

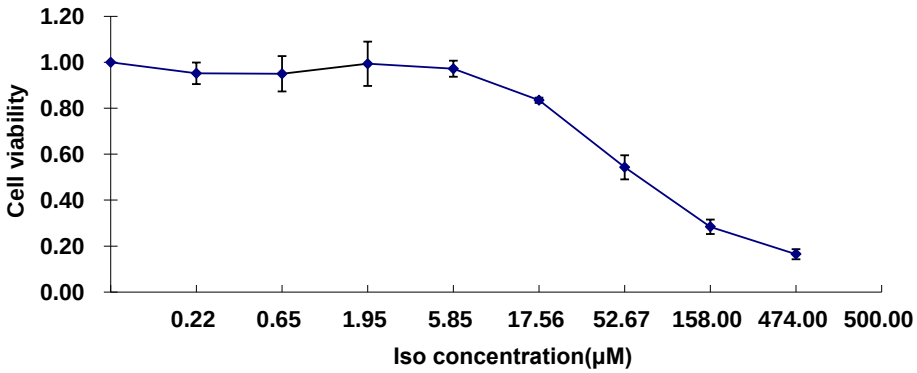

Figure 2. Iso reduces HepG2 cell viability in a dose dependent manner as shown by MTT assay. HepG2 cells were treated with various concentrations of Iso for 48h. Cell viability = [OD (Iso)-OD (blank)] / [OD (control)-OD (blank)]. Data were expressed as means ± SD, n=4.

Iso reduces HepG2 cell viabilities in a dose-dependent way

In order to optimize Iso concentration, a dose-dependent experiment was carried out in HepG2 cells (Figure 2). Cell viability decreased gradually with the increase of Iso concentration. The IC_{50} value of Iso (50 μM) was chosen to treat labelled HepG2 cells for 48 h in the following quantitative analysis.

Protein identification and quantification

To characterize the differentially expressed proteins upon Iso treatment, normal HepG2 cell lysates (Light) and labelled HepG2 cell lysates exposed to 50 μM Iso for 48 h (heavy) were mixed at equal amount (30 μg each) and separated by SDS-PAGE. Each lane of the SDS-PAGE was excised into 25 sections followed by in-gel digestion, and then the samples were analyzed with Agilent 1100 HPLC-Chip/MS system. The average standard deviation (SD) of the isotopic intensity ratios (Light/ Heavy) was 0.7 for all identified proteins. The cut-off ratio was defined as 1.8 (2.5╳SD). Only 84 proteins displayed significant change of their expression level upon Iso treatment. Furthermore, the resulting quantitative proteome had an asymmetric distribution, with 77 proteins down-regulated and 7 proteins up-regulated (Table 1).

Function and location analysis of differential proteins

The significantly changed proteins due to Iso treatment in HepG2 cells were annotated by GO component and biological process (Figure 3A and B). The differential proteins were found to be located in cytoplasm (39%), nucleus (32%) and mitochondria (9.4%). Almost half of the proteins that is 48% are associated with protein synthesis, folding and secretion as well as mRNA processing and transport suggested by function analysis. Proteins accounting for the second large part (14%) are involved in energy-yielding processes such as glycolysis and tricarboxylic acid cycle (TCA), electron transport and ATP synthesis in mitochondria. In addition, 10% of the proteins regulate cell cycle, proliferation and 8% play roles in cell adhesion, and morphogenesis. It was noticed that protein location distribution as shown in Figure 3A is consistent with their functions, for example proteins involved in the regulation of the processes such as protein synthesis, energy production, are located in cytoplasm, nucleus and mitochondria.

Validation of the differential proteins with real-time fluorescence quantitative RT-PCR and Western blotting

Real-time fluorescence quantitative RT-PCR and Western blotting were applied to validate the proteomic results. Four genes: *RBMX, Cdk2, Hsp90, H1b* and three proteins: Cdk2, RBMX, H1b proteins were picked due to their significant change according to SILAC-MS results. *RBMX, Cdk2,* and *Hsp90* were confirmed to be down-regulated as the result of Iso treatment by quantitative RT-PCR assay (Figure 4A). Cdk2, RBMX, H1b protein level in Iso treated HepG2 cells were reduced consistently as shown by Western blotting (Figure 4B). However, reduced H1b protein level accompanied with increased H1b mRNA level suggested post transcriptional mechanisms which played important roles in the regulation of H1b gene expression triggered by Iso treatment.

DISCUSSION

Isorhamnetin, which is also called 3'-O-methylquercetin, is a metabolite of quercetin in plants, as well as in some

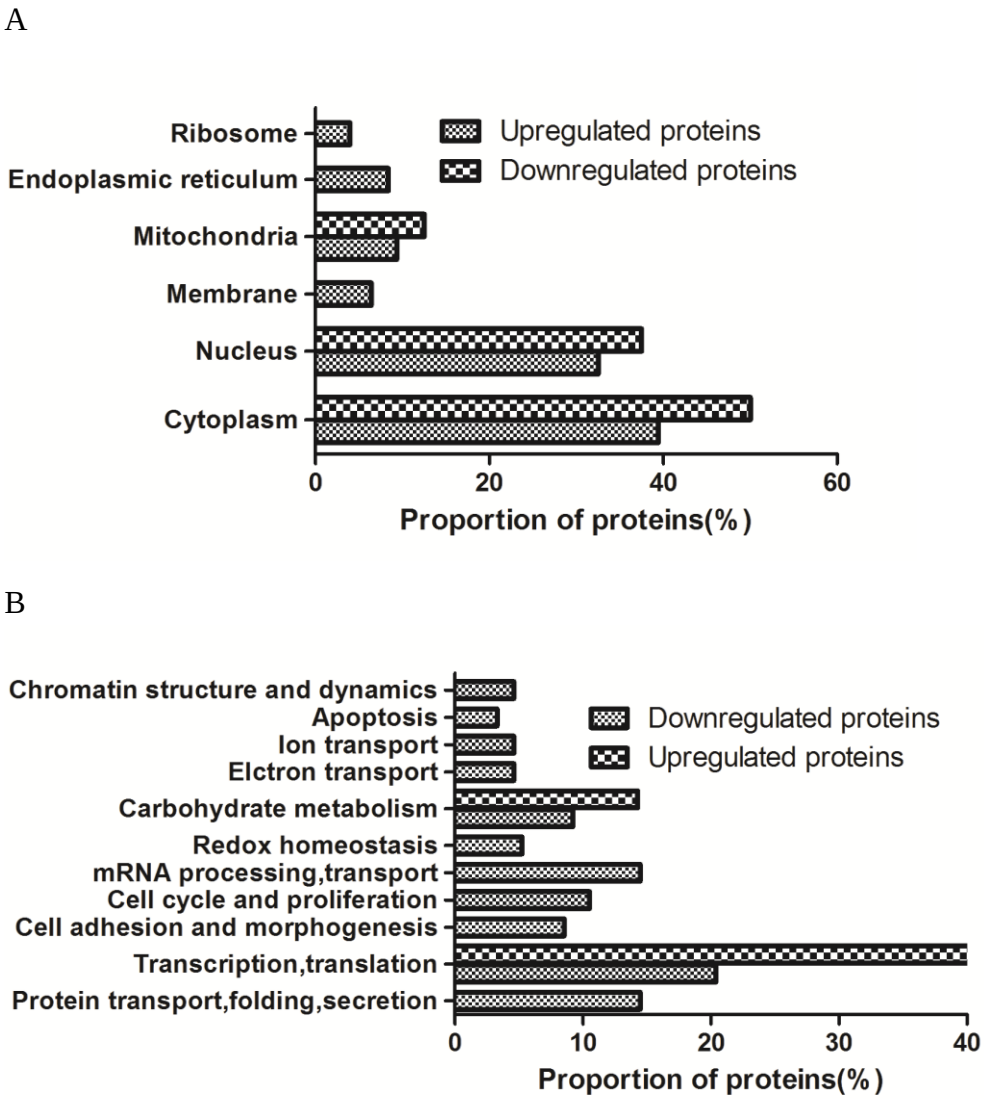

Figure 3. Subcellular localization and function analysis of differential proteins in Iso-treated HepG2 cells based on the annotations of GO. (A) Subcellular localization of differential proteins. (B) Functional distribution of differential proteins.

mammalian species after oral administration. Both quercetin and isorhamnetin exhibited anti-oxidant activities, and have been reported to be protective against oxidative stress-related chronic diseases, including cardiovascular diseases, diabetes, and cancer (Hursting, 1999; Murota and Terao, 2003; Manu et al., 2015; Li et al., 2015; Hu et al., 2015; Ramachandran et al., 2012; Kim et al., 2011; Saud et al., 2013; Jaramillo et al., 2010; Bobe et al., 2008). Iso was capable of enhancing the *in vivo* and *in vitro* anti-tumor effect of capeciatbine in gastric cancer (Manu et al., 2015). Iso inhibited the proliferation and invasion of cancer cells, and induced apoptosis in gastric cancer, but demonstrated minimal effect on the normal cells (Ramachandran et al., 2012). In terms of hepatocellular carcinoma, Iso was found to be cytotoxic at very low doses in contrast to quercetin (Choi et al., 2010). Furthermore, Iso induced apoptosis in BEL-7402 cells, a hepatocellular carcinoma, in a dose- and time- dependent way (Teng et al., 2006).

Previous reports generally focused on single or several related proteins in Iso treated cancer cells (Ma et al., 2007; Lee et al., 2008; Manu et al., 2015; Li et al., 2015; Hu et al., 2015; Ramachandran et al., 2012; Kim et al., 2011; Saud et al., 2013; Jaramillo et al., 2010; Bobe et al., 2008). No studies to our knowledge were focused on the proteomic analysis of Iso effects on hepatocellular carcinoma. Here protein expression profiles of HepG2 cells upon Iso treatment was examined by quantitative approach (SILAC-MS), aiming to obtain some valuable

Table 1. Quantified changed proteins by SILAC-MS.

S/N	Protein name	Downregulated proteins after Iso treatment (Light/Heavy ratio>1)		
		Gene ID	Number of Lys-containing peptides for quantification	Silac ratio*
	Ribosomal proteins			
1	RPLPO-like 60S acidic ribosomal protein PO	220717	4	3.65±1.53
2	RPS17,40S ribosomal protein S17		2	2.92±0.62
3	RPS10, ribosomal protein 10	6204	3	3.80±1.82
5	RPL31	6160	2	4.36±0.71
6	Isoform 1 of nucleolin	4691	18	3.69±2.10
7	NPM,isoform 1 of nucleophosmin	4869	5	3.36±1.09
	mRNA splicing and stability			
8	hnRNPK, heterogeneous nuclear ribonucleoprotein K	3190	12	3.13±1.91
9	FUS,isoform short of RNA binding protein	2521	2	2.59±0.11
10	hnRNPH1	3187	6	3.05±1.38
11	hnRNPA1	144983	2	3.73±0.04
12	CCT5,T-complex protein 1 subunit epsilon	22948	4	3.65±1.10
13	hnRNPD	3184	13	2.80±1.01
14	RBMX, Heterogeneous nuclear ribonucleoprotein G	27316	2	5.62±0.99
15	SNRPD2,small nuclear ribonucleoproein SmD2	6633	3	3.35±0.37
	Factors in transcription and translation process			
16	FUBP,isoform 2 of far upstream element-binding protein 1	8880	2	3.65±2.03
17	EEF1D,eukaryotic translation elongation factor 1	1936	4	3.15±1.43
18	EIF4B, eukaryotic translation initiation factor 4B	1975	2	2.79±0.13
19	EIF3J, eukaryotic translation initiation factor 3 subunit J	8669	2	3.17±0.34
20	YBX2/YBX1,Y-box-binding protein	51087	4	5.94±3.90
21	EEF1B2,elongation factor 1-beta		4	3.31±1.60
22	NPM1,isoform 1 of nucleophosmin	4869	5	3.36±1.09
23	Isoform 1 of nucleolin	4691	18	3.69±2.10
24	AARS,alanyl-tRNA synthetase cytoplasmic	16	3	2.72±0.34
	Transport of amino acid and nucleosome assembly			
25	Isoform A of lamin-A/C	4000	4	2.59±0.97
26	NAP1L1,nucleosome assembly protein 1-like 1	4673	3	4.97±3.39
27	Histon 1.4, Hist1H1E	3008	9	4.67±1.16
28	Histon 1.5, Hist1H1B	3009	2	5.61±0.17

Table 1. Contd.

	Protein folding and secretion			
29	HSP90 AA1(cytosolic), class A member 1 isoform 1	3320	28	2.81±1.34
30	HSP90 B1 endoplasmin precursor	7184	19	3.68±1.22
31	HSPA1A/ HSPA1B	3303/3304	14	3.72±2.06
32	PDIA3,disulfide-isomerase A3 precursor	2923	13	2.63±1.01
33	HSPA9 stress-70 protein, mitochondrial precursor	3313	8	2.57±1.16
34	P4HB, disulfide- isomerase precursor	5034	11	2.43±0.53
35	LRRC59, leucine-rich repeat-containing protein 59	55379	6	4.18±1.85
36	CCT2, T-complex protein 1 subunit beta	10576	9	2.53±1.24
37	M6PRBP1, isoform B of mannose-6-phosphate receptor-binding protein 1	10226	3	2.67±1.32
38	CANX, calnexin precursor	821	4	2.78±1.29
39	PDIA4, disulfide-isomerase A4 precursor	9601	4	2.32±0.76
40	PPIA, peptidyl-prolyl cis-trans isomerase A		4	2.91±0.67
41	STIP1	10963	8	3.20±1.72
42	ERP29, endoplasmic reticulum protein	10961	4	2.44±0.44
43	CCT-8	10694	2	2.52±0.88
44	CCT-6A	908	2	6.11±0.17
45	NACA, nascent polypeptide-associated complex alpha subunit	4666	3	4.23±1.75
46	ST13, Hsc70-interacting protein	6767	3	3.32±0.91
	Metabolism and ATP synthesis			
47	ENO1, isoform alpha-enolase	2023	57	3.87±2.15
48	TPI1, isoform 1 of triosephosphate isomerase	7167	9	2.90±0.82
49	GPI, glucose-6-phosphate isomerase	2821	5	5.27±2.37
50	LDH, L-lactate dehydrogenase	3945	2	5.18±1.70
51	ATP synthase subunit beta, mitochondrial precursor	506	6	3.11±1.01
52	GAPDH	2597	6	4.40±2.53
53	VCP 89KD protein, transitional endoplasmic reticulum ATPase		15	2.98±1.00
54	NME2, nucleoside diphosphate isomerase	4831	7	4.01±1.60
55	ATP5H, isoform 1 of ATP synthase subunit d, mitochondrial precursor	10476	3	3.00±1.03
56	OLA1, isoform 1 of obg-like ATPase	29789	3	3.38±1.31
	Cytoskeletal proteins			
57	Tubulin alpha-1B chain	84790	41	3.80±2.11
58	Keratin, type II cytoskeletal 2 epidermal	3849	8	3.75±1.91

Table 1. Contd.

59	KRT10, keratin type 1 cytoskeletal 10	3858	3	3.65±0.60
60	SLC9A3R, Ezrin-radixin-moesin-binding phosphoprotein 50	9368	3	2.48±0.18
61	Cofilin-1	1072	12	3.48±1.89
62	ITGB1, integrin beta 1	3688	3	4.33±0.51
63	DCTN2, dynactin 2	10540	2	5.08±1.94
	DNA replication and repair, cell cycle			
64	PCNA, proliferating cell nuclear antigen	5111	6	4.18±1.93
65	SET, isoform 1	6418	6	3.11±1.43
66	CDK2, cell division protein kinase 2	983	2	3.42±0.75
67	CAPRINI, caprin-1	4076	2	2.41±0.02
68	RuvB-like 2	10856	3	2.70±0.70
69	CIP29, similar to nuclear protein Hcc-1		2	5.37±2.71
	Redox related proteins			
70	PARK7, protein DJ-1	11315	2	2.92±1.02
71	PRDX1, peroxiredoxin 1	5052	2	2.65±0.42
72	PRDX5	25824	3	3.58±+1.11
73	Glutaredoxin-3	10539	3	3.18±0.91
	Ca^{2+} related proteins and apoptosis			
74	Annexin A1	301	2	4.17±0.12
75	ANXA2, annexin A2 isoform 1	302	3	5.10±2.59
76	CALR, calreticulin precursor	811	4	3.95±1.53
77	API5, isoform 1 of apoptosis inhibitor 5	8539	2	3.18±0.70
	Upregulated proteins after Iso treatment (Light/Heavy ratio<1)			
1	AHNAK, neuroblast differentiation-associated protein	79026	3	0.83±0.57
2	AK2, isoform 1 of adenylate kinase isoenzyme 2, mitochondrial	204	1	0.89
3	TFG, putative MAPK activating protein, TRK-fused gene	10342	1	0.89
4	CKB, creative kinase b-type	1152	1	0.60
5	PSMD11, proteasome 26S non-ATPase subunit 11 variant	5717	1	0.15
6	POLR2D, DNA-directed RNA polymerase II subunit RPB4	5433	1	0.31
7	IGF2BP3, insulin-like growth factor 2 mRNA-binding protein 3	10643	1	0.51

*Silac ratio was expressed as the mean of all peptides for a protein ±SD.

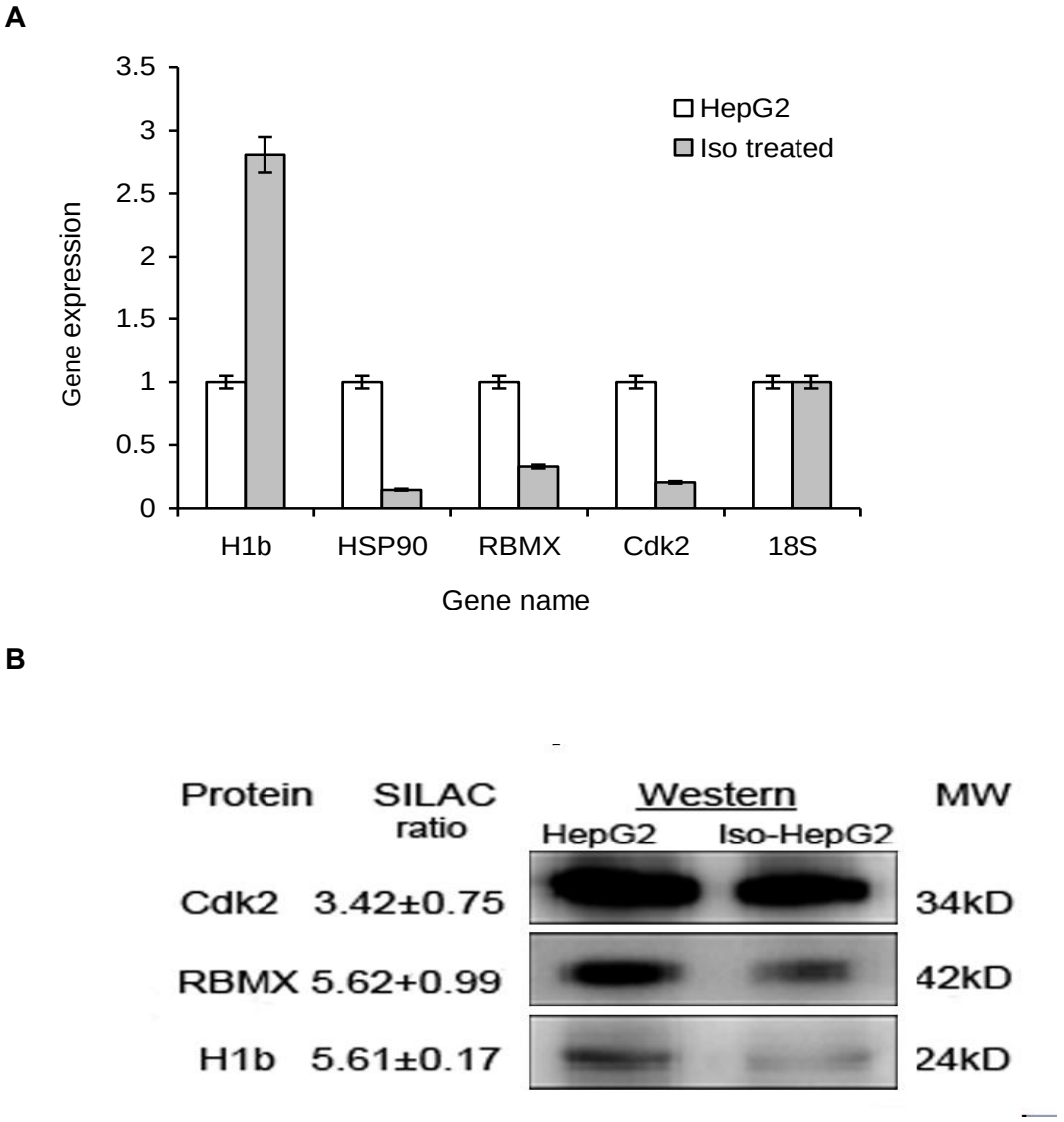

Figure 4. Validation of SILAC-MS results by quantitative RT-PCR and Western blotting. **(A)** Four genes (*H1b, HSP90, RBMX, Cdk2*) which decreased significantly indicated by SILAC-MS were subjected to quantitative RT-PCR. The expression of three genes decreased as expected except H1b gene. **(B)** Proteins including H1b, Cdk2, RBMX were shown to be down-regulated by Western blotting which is consistent with SILAC-MS results.

insights on the anti-cancer mechanisms of Iso. Chaperon proteins, including heat shock protein, T-complex polypeptide accounted for 14% of down-regulated proteins upon Iso treatment, which was similar as quercetin effects in HepG2 cells (Zhou et al., 2009). The downregulation of HSP90 expression upon Iso treatment was further confirmed by quantitative RT-PCR (Figure 4A). Both HSP and CCT are molecular chaperones responsible for the regulation of protein folding to ensure correct conformation, translocation and consequently avoid protein aggregation. Iso was reported to serve as an anticancer agent by degrading oncogenic proteins via downregulation of HSP90 (Mahalingam et al., 2009). Meanwhile Iso was able to induce cancer cell apoptosis and death by down-regulating Hsp90 expression (Zhou et al., 2009; Wei et al., 1994; Yuan et al., 2006; Aalinkeel et al., 2008; Dihal et al., 2008). For example, quercetin down-regulates the expression of Hsp90 which induces cell growth inhibition and cell death in prostate cancer cells while exerting no quantifiable effect on normal prostate epithelial cells (Aalinkeel et al., 2008). Three out of 33 decreased proteins were heat shock proteins in colon mucosa from quercetin fed F344 rats revealed by proteomics technique (Dihal et al., 2008).

Iso affected cell energy metabolism, by decreasing proteins involved in glycolysis and tricarboxylic acid cycle (TCA). Four glycolysis enzymes (α-enolase, triosephophate isomerase, glucose-6-phosphate

isomerase, GAPDH) and two TCA enzymes (fumarate hydratase, acetyl-CoA acetyltransferase) were down-regulated upon Iso treatment, thus resulting in the inhibition of ATP production. Similar results were reported by Dihal that 4 glycolysis enzymes were decreased in colon mucosa, suggesting impaired energy metabolism upon quercetin treatment *in vivo* (Dihal et al., 2008).

The results of Lee et al. (2008) revealed that both anti-proliferation and apoptosis induction mediated anti-tumor activity of Iso in LLC cells. Ma et al. (2007) reported that Iso inhibited cell proliferation and induced apoptosis in Eca-109 cells. Our SILAC-MS findings show that Iso treatment triggered a series of events such as the inhibition of cell energy yields, mRNA processing, DNA repair and cell cycle arrest which are the consequences of cell apoptosis (Table 1). The change of RBMX (related to the mRNA splicing and stability), Cdk2 (cell cycle regulation) expression revealed by SILAC-MS were further validated by quantitative RT-PCR and Western blotting (Figure 4A and B).

Besides apoptosis, Iso also hampered HepG2 cell proliferation through numerous mechanisms at different levels. For instance, ribosomal proteins were decreased. Proteins associated with amino acid transport and nucleosome assembly were also reduced. A significant decline in the amount of H1b and H1e histone illustrates that Iso was able to regulate cell protein synthesis at chromatin level considering the fact that histone H1 could have a regulatory role in gene transcription through the modulation of chromatin folding (Orrego et al., 2007). However, H1b mRNA level was increased while protein level was decreased with Iso treatment in this study, probably owing to negative regulation of H1b expression at post-transcriptional levels, for example translational or post-translational levels.

In contrast to previous studies on quercetin (Zhou et al., 2009), there were some differences on protein profiles of Iso and quercetin. For example, to quercetin, the largest part of the changed proteins (about 23%) were related with signaling transduction, but our largest proportion (20%) were associated with protein synthesis, and few proteins were found to be involved in signaling transduction. The second large part (14%) was chaperon proteins with Iso stimulation, while 7% for quercetin. Regarding subcellular distribution of changed proteins, membrane proteins contained 11% for quercetin, while 6% for Iso. Iso seemed to affect cell metabolism more directly than quercetin since it affected wide range of proteins such as ribosomal proteins, proteins involved in amino acid transport and nucleosome assembly. It is possible that Iso may be more effective than quercetin *in vivo* in cancer therapy although they have similar IC_{50} *in vitro*. Iso significantly suppressed the Lewis lung cancer growth at a dose that is at least one order of magnitude lower than quercetin (Lee et al., 2008). However, these differences may result from different MS assay and amino acid for labelling, for example HPLC-Chip/MS system and lysine for Iso whereas ESI-Quad-TOF and leucine for quercetin, considering that relative abundance of lysine and leucine are different for proteins, but only those peptides containing the labelled amino acid can be quantified.

Conclusion

Iso had profound impacts on HepG2 cells, that is decreased ATP production, inhibition of mRNA process and DNA repair, blockage of cell cycle, affected transport, secretion and folding of the nascent proteins, which were probably due to apoptosis. On the other hand, Iso retarded cell proliferation through weakening protein synthesis in HepG2 cells by inhibiting ribosome assembly, and amino acid transportation. Based on our data, we could predict that anti-proliferation and apoptosis induction mediated anti-tumor activities of Iso.

CONFLICT OF INTERESTS

The authors have not declared any conflict of interests.

ACKNOWLEDGEMENTS

Isorhamnetin was kindly provided by Dr. Jufang Yan from Chengdu Di Ao pharmaceutical group. Protein analysis by Agilent 1100 HPLC-Chip/MS system were performed by Dr. Weifeng He from Chongqing Key Lab for Diseases Proteomics, National Key Lab for Trauma, Burns and Combined Injuries, Institute of Burn Research, Southwest Hospital, Third Military Medical University, Chongqing, People's Republic of China.

REFERENCES

Aalinkeel R, Bindukumar B, Reynolds JL, Sykes DE, Mahajan SD, Chadha KC, Schwartz SA (2008). The dietary bioflavonoid, quercetin, selectively induces apoptosis of prostate cancer cells by down-regulating the expression of heat shock protein 90. Prostate 68(16):1773-1789.

Bobe G, Sansbury LB, Albert PS, Cross AJ, Kahle L, Ashby J, Slattery ML, Caan B, Paskett E, Iber F, Kikendall JW, Lance P, Daston C, Marshall JR, Schatzkin A, Lanza E (2008). Dietary flavonoids and colorectal adenoma recurrence in the Polyp Prevention Trial. Cancer Epidemiol. Biomark. Prev. 17:1344-1353.

Choi KC, Chung WT, Kwon JK, Yu JY, Jang YS, Park SM, Lee SY, Lee JC (2010). Inhibitory effects of quercetin on aflatoxin B1-induced hepatic damage in mice. Food Chem. Toxicol. 48:2747-2753.
component isorhamnetin in vitro inhibits proliferation and induces apoptosis in Eca-109 cells. Chemico-Biol. Interactions 167(2):153-160.

Dihal AA, van der Woude H, Hendriksen PJ, Charif H, Dekker LJ, Ijsselstijn L, de Boer VC, Alink GM, Burgers PC, Rietjens IM, Woutersen RA, Stierum RH (2008). Transcriptome and proteome profiling of colon mucosa from quercetin fed F344 rats point to tumor preventive mechanisms, increased mitochondrial fatty acid degradation and decreased glycolysis. Proteomics 8(1):45-61.

Hibasami H, Mitani A, Katsuzaki H, Imai K, Yoshioka K, Komiya T

(2005). Isolation of five types of flavonol from seabuckthorn (Hippophae rhamnoides) and induction of apoptosis by some of the flavonols in human promyelotic leukemia HL-60 cells. Int. J. Mol. Med. 15(5):805-809.
Hu S, Huang L, Meng L, Sun H, Zhang W, Xu Y (2015). Isorhamnetin inhibits cell proliferation and induces apoptosis in breast cancer via Akt and mitogenactivated protein kinase kinase signaling pathways. Mol. Med. Rep. 12:6745-6751.
Hursting SD, Slaga TJ, Fischer SM, DiGiovanni J, Phang JM (1999). Mechanism-based cancer prevention approaches: Targets, examples, and the use of transgenic mice. J. Natl. Cancer Institute 91(3):215-225.
Jaramillo S, Lopez S, Varela LM, Rodriguez-Arcos R, Jimenez A, Abia R, Guillen R, Muriana FJ (2010). The flavonol isorhamnetin exhibits cytotoxic effects on human colon cancer cells. J. Agric. Food Chem. 58:10869-10875.
Kim JE, Lee DE, Lee KW, Son JE, Seo SK, Li J, Jung SK, Heo YS, Mottamal M, Bode AM, Dong Z, Lee HJ (2011). Isorhamnetin suppresses skin cancer through direct inhibition of MEK1 and PI3-K. Cancer Prev. Res. 4:582-591.
Lee HJ, Lee HJ, Lee EO, Ko SG, Bae HS, Kim CH, Ahn KS, Lu J, Kim SH (2008). Mitochondria-cytochrome C-caspase-9 cascade mediates isorhamnetin-induced apoptosis. Cancer Lett. 270(2):342-353.
Li Q, Ren FQ, Yang CL, Zhou LM, Liu YY, Xiao J, Zhu L, Wang ZG (2015). Anti-proliferation Effects of Isorhamnetin on Lung Cancer Cells *in vitro* and *in vivo*. Asian Pac. J. Cancer Prev. 16:3035-3042.
Ma G, Yang C, Qu Y, Wei H, Zhang T, Zhang N (2007). The flavonoid
Mahalingam D, Swords R, Carew JS, Nawrocki ST, Bhalla K, Giles FJ (2009). Targeting HSP90 for cancer therapy. Br. J. Cancer 100(10):1523-1529.
Manach C, Morand C, Crespy V, Demigné C, Texier O, Régérat F, Rémésy C (1998). Quercetin is recovered in human plasma as conjugated derivatives which retain antioxidant properties. FEBS Lett. 426:331-336.
Manu KA, Shanmugam MK, Ramachandran L, Li F, Siveen KS, Chinnathambi A, Zayed ME, Alharbi SA, Arfuso F, Kumar AP, Ahn KS, Sethi G (2015). Isorhamnetin augments the anti-tumor effect of capeciatbine through the negative regulation of NF-kappaB signaling cascade in gastric cancer. Cancer Lett. 363:28-36.
Morand C, Crespy V, Manach C, Besson C, Demigné C, Rémésy C (1998). Plasma metabolites of quercetin and their antioxidant properties. Am. J. Physiol. 275(1 Pt 2):R212-219.
Murota K, Terao J (2003). Antioxidative flavonoid quercetin: Implication of its intestinal absorption and metabolism. Arch. Biochem. Biophys. 417(1):12-17.
Ong SE, Blagoev B, Kratchmarova I, Kristensen DB, Steen H, Pandey A, Mann M (2002). Stable isotope labeling by amino acids in cell culture, SILAC, as a simple and accurate approach to expression proteomics. Mol. Cell Proteomics 1(5):376-386.
Ong SE, Kratchmarova I, Mann M (2003). Properties of 13Csubstituted arginine in stable isotope labeling by amino acids in cell culture (SILAC). J. Proteome Res. 2:173-181.
Orrego M, Ponte I, Roque A, Buschati N, Mora X, Suau P (2007). Differential affinity of mammalian histone H1 somatic subtypes for DNA and chromatin. BMC Biol. 5:22.
Pan C, Kumar C, Bohl S, Klingmueller U, Mann M (2009). Comparative proteomic phenotyping of cell lines and primary cells to assess preservation of cell type-specific functions. Mol. Cell Proteomics 8:443-450.
Park KH, Choo JJ, Choi SN (2005). Tissue concentrations of quercetin and its metabolite isorhamnetin following oral administration of quercetin in mice. Korean J. Food Sci. Technol. 37(1):90-94.
Patrick AE, Jeroen K, Bruce RZ, Steven PG (2004). Quantitative cancer proteomics: stable isotope labeling with amino acids in cell culture (SILAC) as a tool for prostate cancer research. Mol. Cell Proteomics 3:729-735.
Prokhorova TA, Rigbolt KT, Johansen PT, Henningsen J, Kratchmarova I, Kassem M, Blagoev B (2009). Stable isotope labeling by amino acids in cell culture (SILAC) and quantitative comparison of the membrane proteomes of self-renewing and differentiating human embryonic stem cells. Mol. Cell Proteomics 8:959-970.
Ramachandran L, Manu KA, Shanmugam MK, Li F, Siveen KS, Vali S, Kapoor S, Abbasi T, Surana R, Smoot DT, Ashktorab H, Tan P, Ahn KS, Yap CW, Kumar AP, Sethi G (2012). Isorhamnetin inhibits proliferation and invasion and induces apoptosis through the modulation of peroxisome proliferator-activated receptor gamma activation pathway in gastric cancer. J. Biol. Chem. 287:38028-38040.
Saud SM, Young MR, Jones-Hall YL, Ileva L, Evbuomwan MO, Wise J, Colburn NH, Kim YS, Bobe G (2013). Chemopreventive activity of plant flavonoid isorhamnetin in colorectal cancer is mediated by oncogenic Src and beta-catenin. Cancer Res. 73:5473-5484.
Shimoi K, Yoshizumi K, Kido T, Usui Y, Yumoto T (2003). Absorption and urinary excretion of quercetin, rutin, and alphaG-rutin, a water soluble flavonoid, in rats. J. Agric. Food Chem. 51(9):2785-2789.
Sun Y, Mi W, Cai J, Ying W, Liu F, Lu H, Qiao Y, Jia W, Bi X, Lu N, Liu S, Qian X, Zhao X (2008). Quantitative proteomic signature of liver cancer cells: tissue transglutaminase 2 could be a novel protein candidate of human hepatocellular carcinoma. J. Proteome Res. 7:3847-3859.
Teng BS, Lu YH, Wang ZT, Tao XY, Wei DZ (2006). In vitro anti-tumor activity of isorhamnetin isolated from Hippophae rhamnoides L. against BEL-7402 cells. Pharmacol. Res. 54:186-194.
Wei YQ, Zhao X, Kariya Y, Fukata H, Teshigawara K, Uchida A (1994). Induction of apoptosis by quercetin: involvement of heat shock protein. Cancer Res. 54:4952-4957.
Yuan ZP, Chen LJ, Fan LY, Tang MH, Yang GL, Yang HS, Du XB, Wang GQ, Yao WX, Zhao QM, Ye B, Wang R, Diao P, Zhang W, Wu HB, Zhao X, Wei YQ (2006). Liposomal quercetin efficiently suppresses growth of solid tumors in murine models. Clin. Cancer Res. 12:3193-3199.
Zhou J, Liang S, Fang L, Chen L, Tang M, Xu Y, Fu A, Yang J, Wei YQ (2009). Quantitative proteomics analysis of HepG2 cells treated with quercetin suggests IQGAP1 involved in quercetin-induced regulation of cell proliferation and migration. OMICS A J. Integr. Biol. 13(2):93-103.
Zhu H, Pan S, Gu S, Bradbury EM, Chen X (2002). Amino acid residue specific stable isotope labeling for quantitative proteomics. Rapid Commun. Mass Spectrom 16(22):2115-2123.